Int.J.Curr.Microbiol.App.Sci (2026) *15*(10): 332-339

International Journal of Current Microbiology and Applied Sciences
ISSN: 2319-7706 **Volume 15 Number 10 (2026)**
Journal homepage: http://www.ijcmas.com

Original Research Article https://doi.org/10.20546/ijcmas.2026.1510.036

Steady State CFD Assessment of Airflow in a Portable Laminar Airflow Cabinet Integrated with an Incubator

Kartik Chauhan, Rajesh Chaudhari and Dolatsinh Zala*

GTU-School of Applied Sciences and Technology, Gujarat Technological University, Ahmedabad, Gujarat-382424, India

**Corresponding author*

Keywords

Computational fluid dynamics; laminar airflow cabinet; portable laboratory equipment; integrated incubator; velocity distribution; steady flow.

Article Info

Received:
18 August 2026
Accepted:
30 September 2026
Available Online:
10 October 2026

A B S T R A C T

Integrating a portable laminar airflow cabinet with an incubator offers a compact platform for laboratory work, but the airflow distribution within the shared assembly requires characterization. This study evaluated steady airflow in an integrated cabinet using SOLIDWORKS Flow Simulation 2023. A three-dimensional, laminar-only model was implemented in an external computational domain that included the internal spaces. Air was supplied at a prescribed normal velocity of 0.300 m/s and a temperature of 293.20 K, with an ambient pressure of 101325 Pa. The model contained 257976 reported computational cells, and the calculation proceeded for 128 iterations. Predicted speed ranged from 0 to 0.604 m/s, while the global Z-velocity component ranged from −0.012 to 0.604 m/s. Transverse velocity components remained within approximately ±0.025 m/s. The visualizations showed predominantly forward-directed airflow, with a faster central region and slower peripheral flow. Inlet-surface velocity goals stabilized near 0.300 m/s, indicating consistency with the prescribed boundary condition. The results identify spatial variation that is not captured by the nominal inlet velocity and provide a numerical baseline for selecting downstream measurement locations. Work-area uniformity and predictive accuracy require further evaluation through velocity mapping, mesh sensitivity analysis, and experimental comparison. The findings apply to the modeled airflow condition and do not establish filtration efficiency, microbiological protection, or incubator temperature control.

Introduction

Portable laboratory equipment can reduce the space and installation demands associated with conventional workstations. Integrating an airflow cabinet and an incubator within a single assembly brings sample preparation and incubation into a compact physical arrangement. The value of this configuration depends on the performance of each function within the shared structure. Laboratory design guidance emphasizes selecting facilities and equipment according to the intended activities, operating conditions, and risks (1). Airflow assessment is therefore an essential part of evaluating the working compartment of an integrated cabinet.

A clean-air workstation is designed to deliver filtered air across a defined working region. Its performance depends on the spatial flow field as well as the nominal supply velocity. Wall boundaries, changes in flow area,

and the opening to the surrounding room can alter the downstream velocity distribution. Consequently, a prescribed inlet velocity alone cannot establish the conditions throughout the enclosure. Principles of laminar airflow, high-efficiency particulate air (HEPA) filtration, and equipment testing provide the background for assessing these systems (2).

A laminar airflow clean bench must also be distinguished from a biological safety cabinet. Horizontal clean benches direct filtered air across the work surface toward the operator and are intended for product protection; they do not provide the personnel and environmental containment associated with an appropriately selected biological safety cabinet (3). Similarly, airflow characterization and air-cleanliness classification require different evidence. ISO 14644-1:2015 classifies air cleanliness using airborne particle concentrations, whereas ISO 14644-3:2019 describes performance test methods for cleanrooms and clean zones (4,5). Velocity contours can inform airflow assessment, but cannot establish particle classification or biological containment. Computational fluid dynamics (CFD) provides spatially resolved predictions of velocity and pressure that complement physical measurements. Chen (6) reviewed ventilation prediction methods and discussed the application of CFD to flow conditions that are difficult to characterize using limited point measurements. For an open-front cabinet, relevant quantities include axial and transverse velocity components, the distribution of faster and slower flow, and the interaction between the enclosure and its surroundings. These outputs can guide the placement of measurement planes and probes.

The reliability of CFD predictions depends on the geometry, boundary conditions, mesh resolution, and physical model. Assessment of ventilation models (7) and established procedures for verification, validation, and reporting (8) distinguish numerical convergence from agreement with experimental observations. Grid-refinement methods provide a separate means of estimating discretization uncertainty (9). These distinctions are particularly relevant when monitored goals are located on a prescribed velocity inlet rather than within the downstream working region.

This study characterized steady airflow in a portable cabinet integrated with an incubator at an inlet velocity of 0.300 m/s. The analysis examined inlet-surface goal histories, global velocity and pressure ranges, and spatial airflow patterns. The lower incubator housing was included in the assembly geometry, while active heating and thermal interaction were outside the modeled scope. The objective was to establish a geometry-specific airflow baseline for subsequent measurement and design assessment.

Materials and Methods

Geometry and Computational Domain

The assembly comprised an upper working enclosure with an open front and a lower incubator housing (Figure 1). The CAD model was identified as Part2.SLDPRT, and the simulation project was named Project(1). An external analysis with internal spaces retained was used to include both the enclosure air and the surrounding fluid domain. The reported domain dimensions were approximately 3.447 × 3.605 × 3.770 m in the X, Y, and Z directions, respectively. These dimensions describe the computational domain rather than the physical cabinet. Domain extents and other principal settings are listed in Table 1.

Physical Model and Boundary Conditions

The simulation was performed using SOLIDWORKS Flow Simulation 2023 SP0.0, build 5726. A steady, laminar-only flow model was selected. Gravity, humidity, and solid conduction were disabled, and the initial air velocity was zero in all directions. A normal inlet velocity of 0.300 m/s was prescribed on Face<1>, with the fully developed flow option enabled. The inlet and ambient temperatures were 293.20 K, the reference ambient pressure was 101325 Pa, and the default wall roughness was 0 μm.

The reported maximum Mach number of 1.76×10^{-3} supports an incompressible approximation. For steady, constant-density laminar flow without body forces, the governing equations are:

$$\nabla \cdot u = 0 \quad (1)$$

$$\rho(u \cdot \nabla)u = -\nabla p + \mu \nabla^2 u \quad (2)$$

where u is the velocity vector, p is pressure, ρ is density, and μ is dynamic viscosity. SOLIDWORKS Flow Simulation uses a cell-centered finite-volume formulation (10). Turbulence quantities were not calculated in the laminar-only case.

A characteristic Reynolds number was calculated from

the nominal HEPA filter face dimensions of 1 ft × 1 ft (0.3048 × 0.3048 m). For face width W and height H, the hydraulic diameter was $D_h = 2WH/(W + H) = 0.3048$ m. The filter thickness of 4 inches was not used as the characteristic length. Using U = 0.300 m/s, the converged surface-average air density of 1.20371 kg/m³, and an approximate dynamic viscosity of 1.81×10^{-5} Pa·s at 293.20 K gave:

$$Re = \rho U D_h/\mu = 6080.62 \approx 6.08 \times 10^3 \quad (3)$$

This face-based Reynolds number characterizes the imposed supply condition; it does not independently establish the downstream flow regime in the open cabinet.

Table.1 Principal Computational Settings

Parameter	Setting
Analysis	External with internal spaces retained; steady; laminar only
Fluid and initial state	Air; 293.20 K; 101325 Pa; initial velocity 0 m/s
Inlet	Face<1>; normal velocity 0.300 m/s; fully developed option on
Domain extents X	−1.740 to 1.707 m
Domain extents Y	−1.935 to 1.670 m
Domain extents Z	−1.569 to 2.200 m
Basic mesh dimensions	60 × 62 × 66 cells
Reported mesh counts	Total 257976; fluid 257976; solid 6433; partial 6108
Disabled options	Time dependence, gravity, humidity, solid conduction
Wall roughness	0 µm

Mesh counts are retained as separate software-reported categories and are not summed because their overlap is unspecified.

Numerical monitoring and postprocessing

Two surface goals were defined on Face<1>: average speed and average Z velocity. Both goals were included in the software convergence assessment. The calculation proceeded for 128 iterations and required 861 s on the reported computer. The convergence criteria were $2.43776913 \times 10^{-4}$ m/s for average speed and 3×10^{-9} m/s for average Z velocity; the corresponding reported goal deltas were $1.44814535 \times 10^{-5}$ and $2.22044605 \times 10^{-16}$ m/s. Goal histories were examined together with the global extrema and Z-velocity visualizations. Iteration number represents numerical solution progress rather than physical flow time.

One mesh and one inlet velocity were evaluated. Results were summarized descriptively because the study comprised a deterministic numerical case without experimental replicates. A grid convergence index and measurement-based error estimates were not calculated. Numerical convergence, discretization uncertainty, and experimental validation were treated as distinct aspects of model assessment (8,9)..

Results and Discussion

Inlet surface goal histories

The average-speed goal decreased from approximately 0.311 m/s and approached a plateau after about 40 iterations (Figure 3a). The displayed current and averaged values were 0.300346 and 0.300349 m/s, respectively, with goal achievement indicated at iteration 103. The exported report rounded the final value to 0.300 m/s. The average Z-velocity goal remained at 0.300 m/s (Figure 3b). Because both goals were evaluated on the prescribed velocity inlet, their stability indicates boundary-goal consistency rather than an independent measure of downstream uniformity or whole-domain convergence.

Velocity and pressure ranges

The maximum predicted speed was 0.604 m/s, approximately 2.01 times the prescribed inlet velocity. This ratio compares a local domain maximum with the imposed inlet value rather than two surface averages. The maximum positive Z velocity was also 0.604 m/s. The largest absolute transverse components were 0.022 m/s in X and 0.025 m/s in Y, consistent with predominantly Z-directed motion. These component extrema may occur at different locations and therefore cannot be combined to calculate a local flow angle. Global numerical extrema are summarized in Table 2.

Spatial airflow distribution

The three-dimensional visualization showed airflow trajectories extending from the enclosure toward the open front along the positive global Z direction (Figure 1). The sectional contour showed a faster central band surrounded by slower flow near the upper and lower boundaries and in the exterior region (Figure 2). The

displayed section therefore indicated a spatially varying velocity distribution rather than uniform plug flow.

The minimum Z velocity was −0.012 m/s, corresponding to 4% of the prescribed inlet velocity in magnitude. This value indicates a weak reverse component at some locations within the computational domain. The available extrema do not locate these regions within or outside the working enclosure, so the extent of reverse flow cannot be determined from the reported values alone. The negative contour limit refers to the signed Z component, not to speed.

Pressure and temperature fields

Relative pressure ranged from -1.56×10^{-3} to 4.78×10^{-3} Pa, giving a global span of 6.34×10^{-3} Pa. Absolute pressure was displayed as 101325.00 Pa at both extremes because of the reporting precision. The relative-pressure span describes the modeled domain and should not be interpreted as the filter pressure drop or fan static-pressure requirement. Air temperature remained at 293.20 K throughout the domain, consistent with the isothermal configuration. Active incubator heating was not represented in this case.

Table.2 Global numerical extrema in the computational domain

Quantity	Minimum	Maximum
Speed (m/s)	0	0.604
X velocity (m/s)	−0.019	0.022
Y velocity (m/s)	−0.025	0.023
Z velocity (m/s)	−0.012	0.604
Relative pressure (Pa)	−0.00156	0.00478
Vorticity (s^{-1})	4.70×10^{-8}	19.51
Shear stress (Pa)	0	0.00248
Temperature (K)	293.20	293.20
Density (kg/m^3)	1.20	1.20

Extrema refer to the complete computational domain. Their coordinates and corresponding values restricted to the working region were not available in the exported results.

Airflow characteristics of the integrated cabinet

The simulation predicted predominantly forward-directed airflow with a faster central region and slower peripheral flow. This distribution provides a basis for evaluating how the compact enclosure conveys the imposed supply flow. The relatively small transverse velocity extrema indicate that Z-directed motion dominates the reported velocity components, while the sectional contour shows that central and peripheral conditions should be considered separately when characterizing the working compartment.

The maximum-to-inlet velocity ratio of approximately 2.01 demonstrates that the nominal inlet condition does not describe all local velocities within the domain. The available outputs do not isolate the contributions of geometry, wall effects, or the inlet profile to this difference. The fully developed inlet option may influence the entering distribution. Local profiles and the exact position and area of Face<1> would be needed to attribute the faster central region to a specific mechanism.

The practical contribution of the model is the identification of locations and quantities for subsequent airflow assessment. Measurement planes spanning the central and peripheral regions would help determine how representative the nominal inlet velocity is of the working compartment. Equivalent numerical and experimental quantities should be compared at matched locations, consistent with established approaches to ventilation-model assessment (7).

Numerical interpretation and study limitations

The stable inlet-surface goals show consistency with the imposed boundary condition, but do not independently characterize downstream behavior. Goals on separate work-area planes, signed flow through the open front, and net mass balance across the fluid boundary would provide a stronger assessment of the internal and external flow field. This distinction follows the separation of verification, validation, and reporting described by Chen and Srebric (8).

The laminar-only model is an assumption rather than evidence that the physical cabinet remains laminar under all operating conditions. The filter-face Reynolds number was approximately 6.08×10^3; conventional pipe-flow transition thresholds cannot be directly transferred to this open geometry. Likewise, orderly trajectories do not quantify turbulence. Comparison with an appropriate alternative flow model and matched physical measurements would help assess the sensitivity of the predictions to this assumption.

Figure.1 Three-dimensional airflow visualization of the portable cabinet and lower incubator housing at iteration 128. Trajectories extend toward the open front along positive global Z. The color scale denotes Z velocity (m/s).

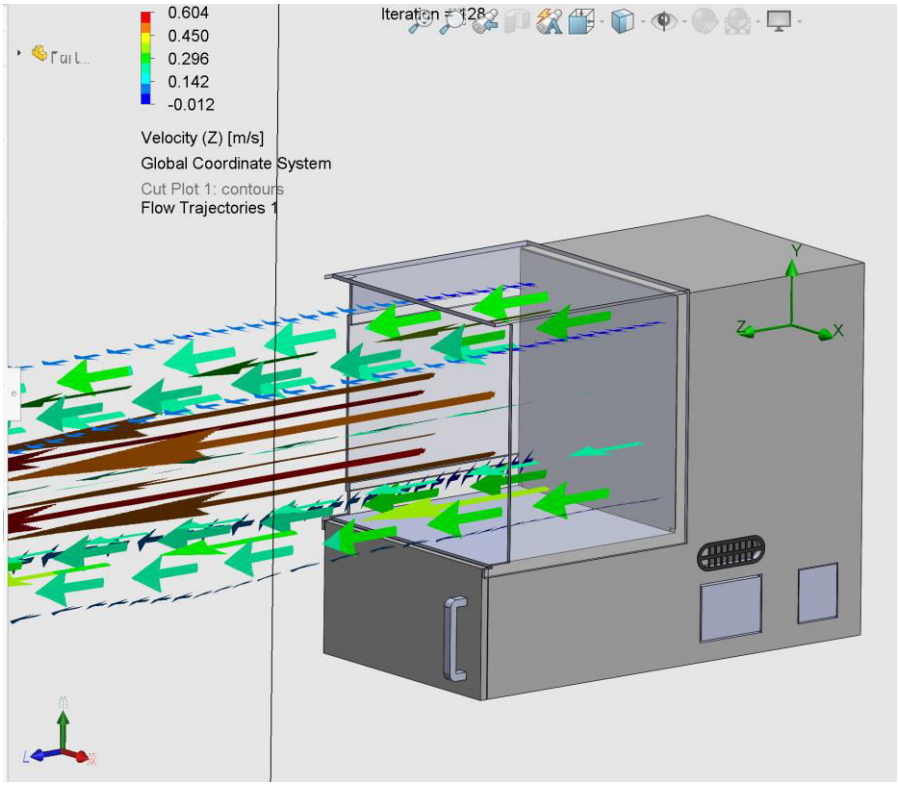


Figure 2. Sectional contour of global Z velocity at iteration 128. A faster central band is surrounded by slower peripheral flow. The color scale ranges from −0.012 to 0.604 m/s; negative values indicate a reverse Z component. The cut-plane coordinates were not specified in the solver export.

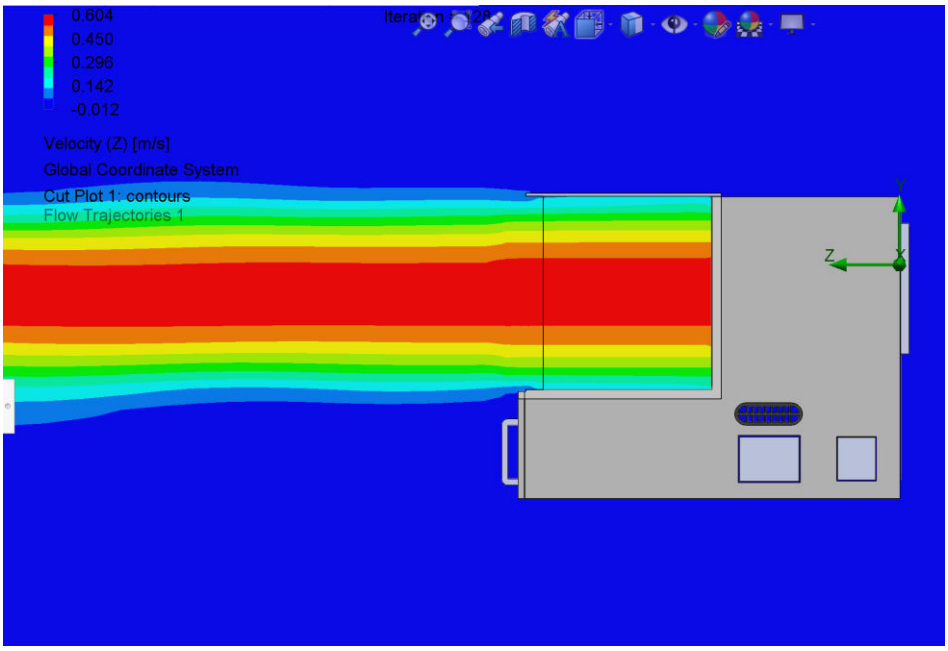


Figure 3a. Iteration history of the average-speed goal on inlet Face<1>. The displayed current and averaged values are 0.300346 and 0.300349 m/s, respectively, with goal achievement indicated at iteration 103.

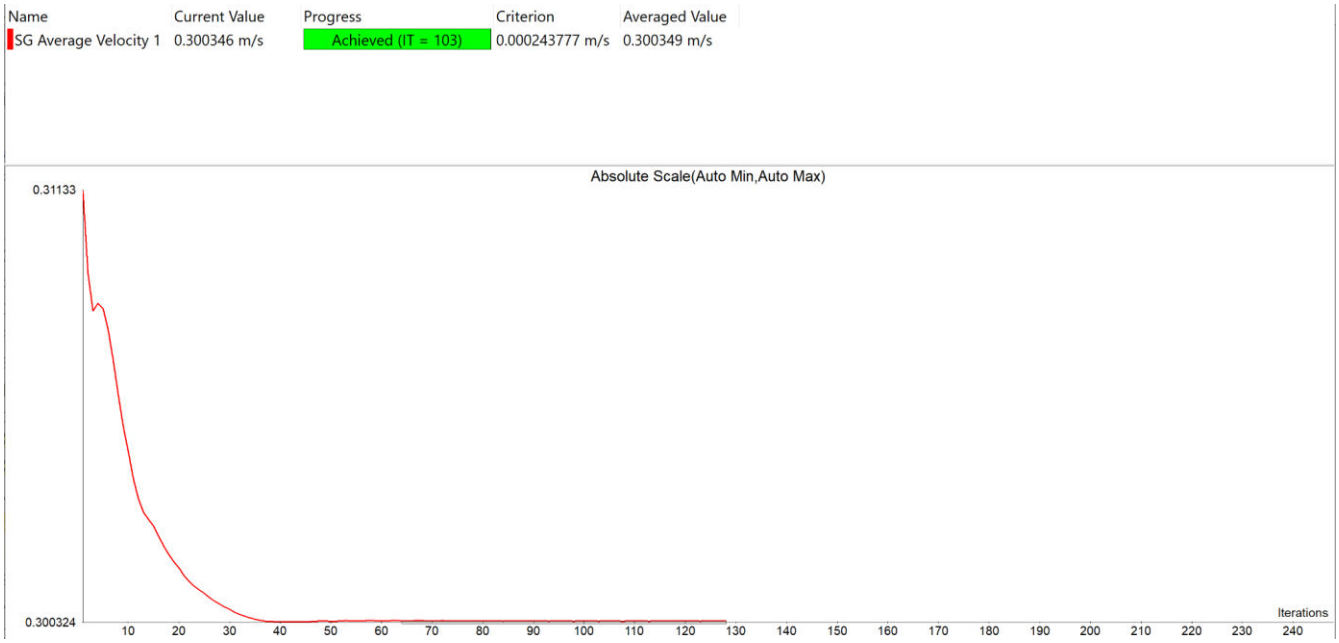
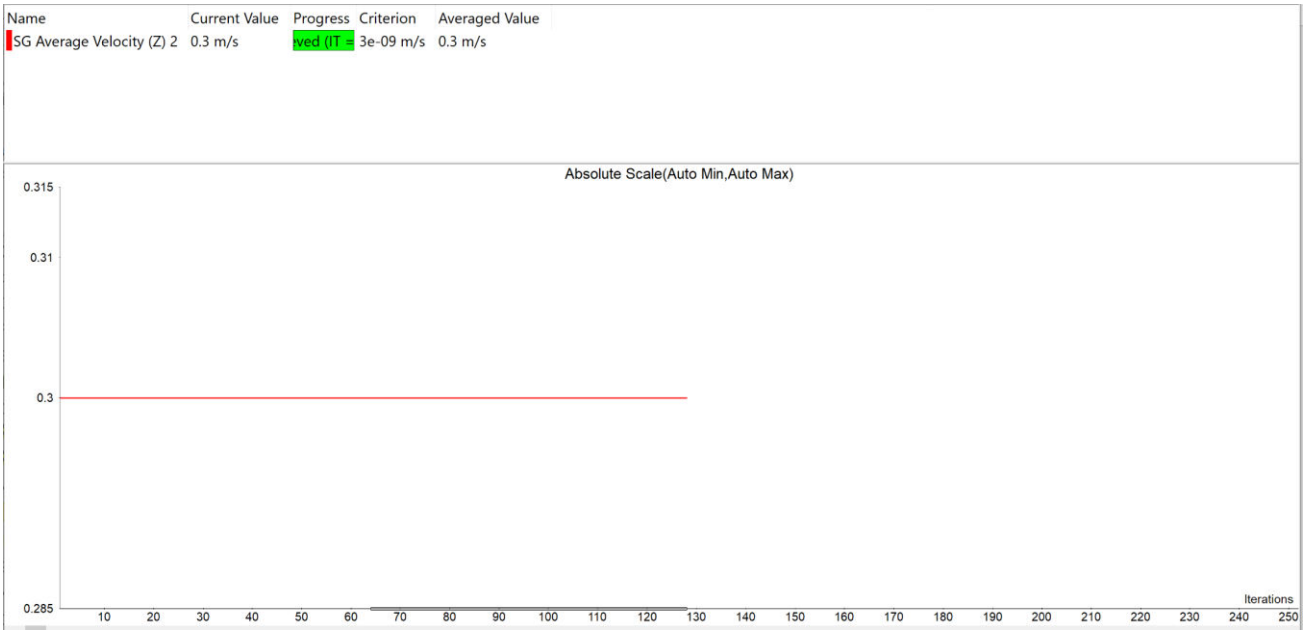


Figure 3b. Iteration history of the average Z-velocity goal on inlet Face<1>. The displayed value remains at 0.300 m/s. In both panels, the horizontal axis denotes numerical iterations; the inlet-surface goals do not independently measure downstream velocity uniformity.



The use of a single mesh and domain limits the assessment of numerical uncertainty. Systematic grid refinement should examine downstream mean velocity, centerline profiles, and reverse-flow extent, following established procedures for discretization-uncertainty estimation (9). Domain-size sensitivity is also relevant

because the calculation includes the surrounding air. These analyses would clarify the robustness of the predicted central acceleration and peripheral velocity gradients.

Experimental validation should map velocities at fixed locations within the enclosure and across the open front under the same operating condition, with measurement uncertainty and repeatability reported. Filter integrity, airborne particle cleanliness, microbiological performance, and incubator temperature uniformity require separate evaluation. In particular, airflow simulation cannot establish ISO air-cleanliness classification (4,5) or the protective functions of a biological safety cabinet (3). The present findings are therefore limited to airflow in the modeled configuration.

In Conclusion, Steady CFD analysis of a portable laminar airflow cabinet integrated with an incubator predicted predominantly forward-directed airflow at a prescribed inlet velocity of 0.300 m/s. The maximum speed was 0.604 m/s, and the displayed section contained a faster central region surrounded by slower peripheral flow. Inlet-surface goals stabilized near the prescribed velocity, while the global Z-velocity minimum of −0.012 m/s indicated a weak reverse component at some domain locations. These results establish a geometry-specific numerical baseline and identify the need to distinguish central and peripheral conditions in subsequent work-area measurements. Downstream velocity extraction, mesh and domain sensitivity analyses, and experimental comparison are required to determine uniformity and predictive accuracy. The conclusions apply to the simulated airflow condition and do not extend to incubator thermal performance or microbiological protection.

Author Contributions

Kartik Chauhan: Investigation, formal analysis, writing—original draft. Rajesh Chaudhari: Validation, methodology, writing—reviewing; Dolatsinh Zala: Formal analysis, writing—review and editing.

Data Availability

The datasets generated during and/or analyzed during the current study are available from the corresponding author on reasonable request.

Declarations

Ethical Approval Not applicable.

Consent to Participate Not applicable.

Consent to Publish Not applicable.

Conflict of Interest The authors declare no competing interests.

References

1. World Health Organization. Laboratory biosafety manual, fourth edition: laboratory design and maintenance. Geneva: World Health Organization; 2020. https://www.who.int/publications/i/item/9789240011397 .
2. Chauhan K, Zala D. Laminar flow and biosafety: essentials for cleanrooms. 1st ed. BP International; 2024. https://doi.org/10.9734/bpi/mono/978-93-48859-52-5
3. Centers for Disease Control and Prevention, National Institutes of Health. Biosafety in microbiological and biomedical laboratories. 6th ed. Meechan PJ, Potts J, editors. U.S. Department of Health and Human Services; 2020.
4. International Organization for Standardization. ISO 14644-1:2015. Cleanrooms and associated controlled environments—Part 1: classification of air cleanliness by particle concentration. Geneva: ISO; 2015. https://www.iso.org/standard/53394.html.
5. International Organization for Standardization. ISO 14644-3:2019. Cleanrooms and associated controlled environments—Part 3: test methods. Geneva: ISO; 2019. Corrected version 2020-06. https://www.iso.org/standard/60598.html.
6. Chen Q. Ventilation performance prediction for buildings: a method overview and recent applications. Building and Environment. 2009;44(4):848–858. https://doi.org/10.1016/j.buildenv.2008.05.025
7. Chen Q, Lee K, Mazumdar S, Poussou S, Wang L, Wang M, Zhang Z. Ventilation performance prediction for buildings: model assessment. Building and Environment. 2010;45(2):295–303. https://doi.org/10.1016/j.buildenv.2009.06.008
8. Chen Q, Srebric J. A procedure for verification, validation, and reporting of indoor environment CFD

analyses. HVAC&R Research. 2002;8(2):201–216. https://doi.org/10.1080/10789669.2002.10391437

9. Celik IB, Ghia U, Roache PJ, Freitas CJ, Coleman H, Raad PE. Procedure for estimation and reporting of uncertainty due to discretization in CFD applications. Journal of Fluids Engineering. 2008;130(7):078001. https://doi.org/10.1115/1.2960953.
10. Dassault Systèmes SolidWorks Corporation. An introduction to flow analysis applications with SolidWorks Flow Simulation: instructor guide. SolidWorks 2011 edition. Concord, MA: Dassault Systèmes SolidWorks Corporation; 2011. https://www.solidworks.com/sw/docs/Flow_Sim_InstructorWB_2011_ENG.pdf.

How to cite this article:

Kartik Chauhan, Rajesh Chaudhari and Dolatsinh Zala. 2026. Steady State CFD Assessment of Airflow in a Portable Laminar Airflow Cabinet Integrated with an Incubator. *Int.J.Curr.Microbiol.App.Sci.* 15(10): 332-339.
doi: https://doi.org/10.20546/ijcmas.2026.1510.036